Available online at www.sciencedirect.com

ScienceDirect

IFAC Papers Online CONFERENCE PAPER ARCHIVE

IFAC PapersOnLine 52-16 (2019) 771–776

A First-Order Differentiator with First-Order Sliding Mode Filtering

Ryo Kikuuwe * **Rainhart Pasaribu** ** **Gyuho Byun** ***

* *Hiroshima University, Higashi-Hiroshima 739-8527, Japan (e-mail: kikuuwe@hiroshima-u.ac.jp).*
** *Institut Teknologi Bandung, Bandung 40132, Indonesia.*
*** *Kyushu University, Fukuoka 819-0395, Japan.*

Abstract: This paper proposes a sliding mode differentiator for estimating the first-order derivatives of noisy signals. The proposed differentiator can be seen as a version of Slotine et al.'s sliding mode observer extended with additional non-Lipschitzness. It behaves exactly as a first-order low-pass filter in the sliding mode and is globally convergent. Its discrete-time implementation is based on the implicit (backward) Euler discretization, which does not result in chattering. The differentiator is validated through some numerical examples.

Keywords: Sliding mode observer, Differentiator, Implicit Euler discretization, Noise filtering

1. INTRODUCTION

In many control applications, numerical differentiation of sensor signals, which are usually noisy, is an important issue. An estimation problem of signal derivatives can be formulated as an observation problem of a simple integrator of which the input is not available and the output is contaminated by noise. The most straightforward way is Euler differentiation combined with a linear low-pass filter (LPF), which can also be seen as a Luenberger observer of an integrator (Vasiljevic and Khalil, 2008). Some researchers have studied the use of sliding-mode observers for estimating signal derivatives. One example is Slotine et al.'s (1987) first-order sliding-mode observer, in which $s = 0$ is intended to be achieved where s is the sliding variable. It involves a discontinuous function, which usually needs to be approximated through a boundary-layer approach in the implementation. Other researchers use higher-order sliding mode observers (Levant, 1998, 2003; Davila et al., 2005; Iqbal et al., 2010), with which the higher-order time derivatives of s are maintained continuous.

In the context of observation problems, Vasiljevic and Khalil (2008) analyzed the upperbound of the estimation error under bounded measurement noise. Effects of noise on sliding mode observers have been discussed with boundary-layer approximations (Slotine et al., 1987; Moura et al., 1997) and with Lipschitz assumptions on the noise (Levant, 2003). Because it is in principle impossible to distinguish the signal component and the noise components in the input signal, the observer design always requires a certain level of a priori knowledge or assumptions. In the design of linear LPFs, one usually adjusts the cut-off frequency to obtain appropriately smooth outputs. In contrast, in the design of sliding mode differentiators, the upperbound of the signal derivatives need to be taken into consideration (Vázquez et al., 2016; Levant and Livne, 2012). Another important difference is that the global convergence is trivially realized in the case of linear LPFs but needs careful parameter design in the case of sliding mode differentiators.

This paper proposes a new sliding mode differentiator to obtain the first-order derivative of noisy signals. Its structure can be seen as a first-order sliding mode system similar to Slotine et al.'s (1987) observer but it includes a non-Lipschitz function. The new differentiator behaves exactly as a first-order LPF in the sliding mode and as a second-order LPF when it is far from the sliding mode. Due to this property, its behavior is in the middle between the first and second-order LPFs, having a certain balance between the noise attenuation and the signal preservation. The non-Lipschitz term is intended to realize smooth transition between the sliding mode and the reaching mode. The global asymptotic stability in the unperturbed case and the global input-to-state stability are proven. This paper also presents a discrete-time implementation of the new differentiator based on the implicit (backward) Euler discretization, which prevents chattering.

The rest of this paper is organized as follows. Section 2 presents a new differentiator structure, which is a non-Lipschitz variant of Slotine-type observer, and some analyses on its behaviors. Section 3 presents its discrete-time implementation. Section 4 shows some experimental results. Section 5 provides concluding remarks.

2. NEW DIFFERENTIATOR

2.1 The Structure

Let us consider the following system:

$$\dot{x}_1 = x_2 \tag{1a}$$

$$\dot{x}_2 = u \tag{1b}$$

$$y = x_1 + v \tag{1c}$$

where x_1 and x_2 are state variables and u is an unknown input. The output y is the measured value that

2405-8963
Peer review under responsibility of International Federation of Automatic Control.
10.1016/j.ifacol.2019.12.056

is corrupted with the unknown noise v. This system is a simple second-order integrator of an unknown input signal u. The problem considered in this paper is to construct an observer to estimate the state variable x_2 from the measured system output y. Such an observer can be seen as a first-order differentiator of the noisy signal y. It should be noted that the system (1) does not represent a particular physical system but represents an imaginary system, of which the unknown states x_1 and x_2 are the "true" values of the noisy measurement y and its derivative, respectively. Here we assume that y and u are differentiable with respect to time.

For the system (1), we consider the following observer:

$$\begin{bmatrix} \dot{z}_1 \\ \dot{z}_2 \end{bmatrix} \in \begin{bmatrix} z_2 - \kappa_1(z_1 - y) \\ -\kappa_2(z_1 - y) \end{bmatrix} - \begin{bmatrix} \alpha_1 \\ \alpha_2 \end{bmatrix} \eta(z_1 - y) \quad (2a)$$

$$w = z_2. \quad (2b)$$

Here, z_1 and z_2 are the estimated values of x_1 and x_2, respectively, w is the output of the observer, and $\{\kappa_1, \alpha_1, \kappa_2, \alpha_2\}$ are non-negative constants. The function η is a set-valued function (it is why (2) is a differential inclusion) that satisfies the following conditions:

$$\eta(0) = [-1, 1] \quad (3a)$$

$$\lim_{\xi \searrow 0} \eta(\xi) = 1, \ \lim_{\xi \nearrow 0} \eta(\xi) = -1 \quad (3b)$$

$$\eta'(\xi) \geq 0 \ \forall \xi \neq 0 \quad (3c)$$

$$\lim_{\xi \to \pm\infty} \eta(\xi)/\xi = 0 \quad (3d)$$

$$\lim_{\xi \searrow 0} \eta'(\xi) = \lim_{\xi \nearrow 0} \eta'(\xi) = \infty \quad (3e)$$

$$\lim_{\xi \to \pm\infty} \eta(\xi) = \pm\infty. \quad (3f)$$

The properties (3a) and (3b) suggest that η is a continuous (both upper and lower semicontinuous) set-valued map (Cortés, 2008, p.49). The property (3c) implies that η is monotonic. The property (3e) means that η is non-Lipschitz.

If one neglects the conditions (3e)(3f), one choice for the function η is the set-valued signum function that is defined as follows:

$$\mathrm{sgn}(\xi) \triangleq \begin{cases} \xi/|\xi| & \text{if } \xi \neq 0 \\ [-1, 1] & \text{if } \xi = 0. \end{cases} \quad (4)$$

In this case, the structure (2) reduces to Slotine et al.'s (1987) observer applied to the plant (1). It is also obvious that setting $\alpha_1 = \alpha_2 = 0$ reduces (2) into the Luenberger observer whose transfer function is $\kappa_2 s/(s^2 + \kappa_1 s + \kappa_2)$, which is a first-order differentiator combined with a second-order LPF, and the one referred to as a high-gain observer by Vasiljevic and Khalil (2008). The non-Lipschitz term $\eta(z_1 - y)$ may have some similarity to fractional power terms that appear in Levant's (2003) higher-order sliding mode differentiator.

When the observer (2) is applied to the system (1), the following system is obtained:

$$\dot{\boldsymbol{e}} \in \boldsymbol{A}\boldsymbol{e} - \boldsymbol{\alpha}\eta(e_1) - \boldsymbol{v} \quad (5)$$

where $\boldsymbol{v} \triangleq [\dot{v}, u]^T$, $\boldsymbol{\alpha} \triangleq [\alpha_1, \alpha_2]^T$,

$$\boldsymbol{A} \triangleq \begin{bmatrix} -\kappa_1 & 1 \\ -\kappa_2 & 0 \end{bmatrix} \quad (6)$$

$$\boldsymbol{e} \triangleq [e_1, e_2]^T \triangleq [z_1 - y, w - x_2]^T. \quad (7)$$

Here, the state variable e_1 is not exactly an estimation error, but is the one including the effect of the measurement noise v. In contrast, e_2 is defined with excluding the noise component $\dot{v}$ because the aim of this observer is to achieve $e_2 = z_2 - x_2 \to 0$.

2.2 Stability and Rechability

Stability properties of the error system (5) are now discussed.

Theorem 1. With the system (5) in which $\boldsymbol{v} \equiv 0$, the origin is globally asymptotically stable.

Proof. Let us define the following Lyapunov function candidate:

$$V(\boldsymbol{e}) = \boldsymbol{e}^T \boldsymbol{P} \boldsymbol{e}/2 + \mu\hat{\eta}(e_1) \quad (8)$$

where $\hat{\eta}$ is a function defined by $d\hat{\eta}(\xi)/d\xi = \eta(\xi)$ and $\hat{\eta}(0) = 0$,

$$\boldsymbol{P} \triangleq \begin{bmatrix} 1 & -\beta \\ -\beta & 1/\kappa_2 \end{bmatrix} \quad (9)$$

$$\mu \triangleq \alpha_1 \left(\alpha_2/(\alpha_1\kappa_2) - \beta\right), \quad (10)$$

and β is a positive constant. Then, the following is obtained:

$$\begin{aligned} \dot{V}(\boldsymbol{e}) &= (\boldsymbol{e}^T\boldsymbol{P} + \eta(e_1)[\mu, 0])(\boldsymbol{A}\boldsymbol{e} - \boldsymbol{\alpha}\eta(e_1) - \boldsymbol{v}) \\ &= -\boldsymbol{e}^T\boldsymbol{Q}\boldsymbol{e} - \mu_c e_1 \eta(e_1) - \alpha_1 \mu \eta(e_1)^2 \\ &\quad -\boldsymbol{e}^T\boldsymbol{P}\boldsymbol{v} - \mu\eta(e_1)\dot{v} \end{aligned} \quad (11)$$

where

$$\boldsymbol{Q} \triangleq -\frac{1}{2}(\boldsymbol{P}\boldsymbol{A} + \boldsymbol{A}^T\boldsymbol{P}) = \begin{bmatrix} \kappa_1 - \beta\kappa_2 & -\beta\kappa_1/2 \\ -\beta\kappa_1/2 & \beta \end{bmatrix} \quad (12)$$

$$\mu_c \triangleq (\alpha_1\kappa_1 + \alpha_2)\left(\frac{\alpha_1\kappa_2 + \alpha_2\kappa_1}{\kappa_2(\alpha_1\kappa_1 + \alpha_2)} - \beta\right). \quad (13)$$

Therefore, by choosing β such that it satisfies

$$0 < \beta < \min\left(\frac{4\kappa_1}{\kappa_1^2 + 4\kappa_2}, \frac{1}{\sqrt{\kappa_2}}, \frac{\alpha_2}{\alpha_1\kappa_2}, \frac{\alpha_1\kappa_2 + \alpha_2\kappa_1}{\kappa_2(\alpha_1\kappa_1 + \alpha_2)}\right), \quad (14)$$

$V(\boldsymbol{e})$ is positive definite and $\dot{V}(\boldsymbol{e})$ is negative definite with $\boldsymbol{v} \equiv 0$. That is, with $\boldsymbol{v} \equiv 0$, the origin is globally asymptotically stable.

Theorem 2. The system (5) is globally input-to-state stable with respect to the input $\boldsymbol{v}$.

Proof. Now we use the Lyapunov function V defined by (8). If β satisfies (14), (11) shows that the following is satisfied:

$$\dot{V}(\boldsymbol{e}) < -\lambda_Q \|\boldsymbol{e}\|^2 + (\gamma_P\|\boldsymbol{e}\| + \mu\eta(e_1))\|\boldsymbol{v}\| \quad (15)$$

where $\lambda_Q > 0$ is the minimum eigenvalue of $\boldsymbol{Q}$ and $\gamma_P > 0$ is the maximum eigenvalue of $\boldsymbol{P}$. Therefore, if there exists an upperbound L of $\|\boldsymbol{v}\|$, $\dot{V}(\boldsymbol{e}) < 0$ is satisfied for all $\boldsymbol{e} \in \mathbb{R}^2$ outside the subset $\mathcal{E}$ that is defined as follows:

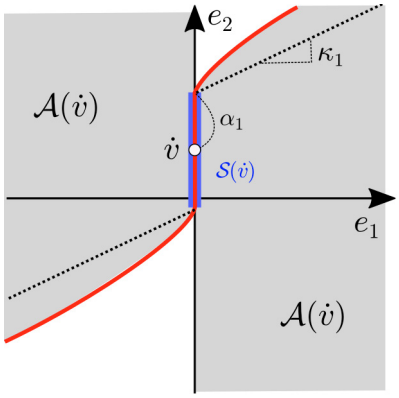

Fig. 1. The sliding patch $\mathcal{S}(\dot{v})$ and the region of direct attraction $\mathcal{A}(\dot{v})$ in the error state space.

$$\mathcal{E} \triangleq \left\{ \boldsymbol{e} \in \mathbb{R}^2 \;\middle|\; \lambda_Q \|\boldsymbol{e}\| - L\left(\gamma_P + \frac{\mu\eta(e_1)}{\|\boldsymbol{e}\|}\right) \le 0 \right\}, \quad (16)$$

which is a closed set including the origin in its interior. Such a set $\mathcal{E}$ exists for any $L > 0$. This implies that, for any $\boldsymbol{v}$ satisfying $\|\boldsymbol{v}\| \le L$ and for any initial states, the state $\boldsymbol{e}$ converges to an ultimate bound, which is a level set of $V(\boldsymbol{e})$ including $\mathcal{E}$. Therefore, the system is globally input-to-state stable. □

As the effect of the set-valuedness of the term $\eta(e_1)$, the system (5) can be in a sliding mode on the surface $e_1 = 0$. The following theorem shows this fact:

Theorem 3. With the system (5), the sliding mode is established on a subset of the subspace $e_1 = 0$ of the state space.

Proof. When $e_1 \neq 0$, the following is satisfied:

$$\frac{de_1^2}{dt} = -2e_1(\kappa_1 e_1 + \alpha_1\eta(e_1) + \dot{v} - e_2). \quad (17)$$

The properties (3a)(3b)(3c) of η imply that, if $\boldsymbol{e}$ is in the subset

$$\mathcal{A}(\dot{v}) \triangleq \left\{ \boldsymbol{e} \in \mathbb{R}^2 \,\middle|\, e_1(\kappa_1 e_1 + \alpha_1\eta(e_1) + \dot{v} - e_2) > 0 \right\}, \quad (18)$$

there exists a $\varepsilon > 0$ with which $de_1^2/dt < -\varepsilon|e_1|$ is satisfied. One can see that $\mathcal{A}(\dot{v})$ covers a neighborhood of the following subset:

$$\mathcal{S}(\dot{v}) \triangleq \{\boldsymbol{e} \in \mathbb{R}^2 \,|\, e_1 = 0 \wedge |e_2 - \dot{v}| < \alpha_1\}, \quad (19)$$

which is a subset of the subspace $e_1 = 0$. Therefore, one can see the sliding mode is established on $\mathcal{S}(\dot{v})$. □

The subset $\mathcal{S}(\dot{v})$ can be referred to as a "sliding patch," and the subset $\mathcal{A}(\dot{v})$ can be referred to as a "region of direct attraction" (Slotine et al., 1987, Section 2.3). Fig. 1 illustrates these subsets in the e_1-e_2 state space. These subsets move in the vertical direction in the figure according to the noise derivative $\dot{v}$. As long as the state $\boldsymbol{e}$ stays in the set $\mathcal{A}(\dot{v})$, the state approaches to the subspace $e_1 = 0$. The state $\boldsymbol{e}$ may go out of the set $\mathcal{A}(\dot{v})$ before reaching the subspace $e_1 = 0$, but Theorem 2 guarantees that the state eventually converges to a neighborhood of the origin.

2.3 Behavior in the Sliding Mode

When the error state $\boldsymbol{e}$ is on the sliding patch $\mathcal{S}(\dot{v})$, $y = z_1$ and $\dot{y} = \dot{z}_1$ are satisfied and thus the observer (2) reduces to the following form:

$$\dot{y} = w - \alpha_1\sigma, \quad \dot{w} = -\alpha_2\sigma, \quad |\sigma| \le 1, \quad (20)$$

which is equivalent to the following:

$$\dot{w} = \alpha_2(\dot{y} - w)/\alpha_1 \quad (21a)$$

$$|w - \dot{y}| \le \alpha_1. \quad (21b)$$

Here, (21a) can also be rewritten as follows:

$$\mathcal{L}[w] = sG_{\mathrm{sm}}(s)\mathcal{L}[y] \quad (22a)$$

where

$$G_{\mathrm{sm}}(s) \triangleq \alpha_2/(\alpha_1 s + \alpha_2). \quad (22b)$$

That is, the observer (2) behaves as a first-order LPF $G_{\mathrm{sm}}(s)$, from $\dot{y}$ to w. The influence of the measurement noise $\dot{v}$ is reduced by $G_{\mathrm{sm}}(s)$, as long as $|w - \dot{y}| \le \alpha_1$.

2.4 Behavior outside the Sliding Mode

With vectors $\boldsymbol{e}_o = [e_{o1}, e_{o2}]^T$ and $\boldsymbol{e} = [e_1, e_2]^T$, if $\boldsymbol{e}_o$ and $\boldsymbol{e}$ are close enough to each other and $e_1 e_{o1} > 0$, the following is satisfied:

$$\eta(e_1) \approx \eta(e_{o1}) + \eta'(e_{o1})(e_1 - e_{o1}) \quad (23)$$

because of the continuity of η. In this case, the system (5) can be approximated as follows:

$$\dot{\boldsymbol{e}} \approx \begin{bmatrix} -\kappa_1 - \alpha_1\eta'(e_{o1}) & 1 \\ -\kappa_2 - \alpha_2\eta'(e_{o1}) & 0 \end{bmatrix} (\boldsymbol{e} - \boldsymbol{e}_o) + \boldsymbol{A}\boldsymbol{e}_o - \boldsymbol{\alpha}\eta(e_{o1}) - \boldsymbol{v}. \quad (24)$$

If one choose $\boldsymbol{e}_o$ so that

$$\boldsymbol{v} \in \boldsymbol{A}\boldsymbol{e}_o - \boldsymbol{\alpha}\eta(e_{o1}) \quad (25)$$

is satisfied, the following is satisfied:

$$\dot{\boldsymbol{e}} \approx \begin{bmatrix} -\kappa_1 - \alpha_1\eta'(e_{o1}) & 1 \\ -\kappa_2 - \alpha_2\eta'(e_{o1}) & 0 \end{bmatrix} (\boldsymbol{e} - \boldsymbol{e}_o). \quad (26)$$

In this case, for an infinitisimal time period, the system can be seen as a linear system with the equilibrium $\boldsymbol{e}_o$.

By observing the eigenvalues of the 2×2 matrix in (26), one can see that the locations of the system poles continuously vary according to e_{o1} from $\{(-\kappa_1 \pm \sqrt{\kappa_1^2 - 4\kappa_2})/2\}$ to $\{-\alpha_2/\alpha_1, -\infty\}$ as e_{o1} approaches to zero because $\eta'(e_{o1})$ is not upperbounded. This is consistent with the fact that, when the system is in the sliding mode at e_{o1}, the system has a pole at $-\alpha_2/\alpha_1$, as suggested by (22). If $\eta'(e_{o1})$ is upperbounded (i.e., if η is Lipschitz and if (3e) is not satisfied), the poles would not reach $\{-\alpha_2/\alpha_1, -\infty\}$ as long as $e_{o1} \neq 0$ but would discontinuously jump from a certain value to $-\alpha_2/\alpha_1$ when it reaches $e_{o1} = 0$. This point supports the importance of the property (3e), the non-Lipschitzness, of η.

Another observation can be obtained regarding the property (3f), the unboundedness, of η. If η is bounded, (25)

implies that $\|\boldsymbol{e}_o\|$ linearly increases as $\boldsymbol{v}$ increases, but the unboundedness of η results in smaller $\|\eta_o\|$, which results in smaller influence of the input $\boldsymbol{v}$ to the error state $\boldsymbol{e}$.

When $|e_1|$ is very large, i.e., when the system (5) is very far from the sliding mode, the term $\boldsymbol{Ae}$ becomes dominant over the term $\boldsymbol{\alpha}\eta(e_1)$. In such a case, the system (5) is close to the linear system $\dot{\boldsymbol{e}} \approx \boldsymbol{Ae} - \boldsymbol{v}$, which results in the following:

$$\mathcal{L}[w] \approx sG_{\rm far}(s)\mathcal{L}[y] \tag{27}$$

where

$$G_{\rm far}(s) \triangleq \kappa_2/(s^2 + \kappa_1 s + \kappa_2). \tag{28}$$

That is, the observer (2) becomes close to the second-order LPF $G_{\rm far}(s)$, from $\dot{y}$ to w, and the influence of the measurement noise $\dot{v}$ is reduced by $G_{\rm far}(s)$.

2.5 Choice of α_i and κ_i: Cut-off Frequencies and Threshold

Previous sections have shown that the observer (2) behaves as a first-order LPF, $G_{\rm sm}(s)$, in the sliding mode and becomes closer to a second-order LPF, $G_{\rm far}(s)$, in a faraway region from the sliding mode. In order to keep e_2 small, one reasonable way is to employ the following settings:

$$\{\alpha_1, \alpha_2\} = \{\gamma, \gamma\omega_{\rm sm}\} \tag{29a}$$
$$\{\kappa_1, \kappa_2\} = \{2\omega_{\rm far}, \omega_{\rm far}^2\} \tag{29b}$$

where $\gamma = \alpha_1$ is an appropriately chosen threshold value on $|e_2 - \dot{v}|$, which defines the size of the sliding patch $\mathcal{S}(\dot{v})$, and $\omega_{\rm sm}$ and $\omega_{\rm far}$ are appropriately low cut-off frequencies. Because the observer (2) behaves as $G_{\rm sm}(s)$ as long as $|e_2 - \dot{v}| \le \gamma$, the value of γ should be chosen as the upperbound of $|e_2 - \dot{v}|$ under which the filtering performance of $G_{\rm sm}(s)$ is acceptable. When $|e_2 - \dot{v}| > \gamma$, the observer (2) should provide stronger filtering effect than $G_{\rm sm}(s)$. Therefore, the filtering effect of $G_{\rm far}(s)$ should be set stronger than $G_{\rm sm}(s)$. With the same cut-off frequency, the filtering effect of $G_{\rm far}(s)$, which is of the second order, is stronger than $G_{\rm sm}(s)$, which is of the first order. Therefore, it is reasonable to choose $\omega_{\rm sm} = \omega_{\rm far}$.

3. DISCRETE-TIME IMPLEMENTATION

For the implementation to digital computers, the continuous-time representation (2) needs to be appropriately discretized. A direct use of the discontinuous function η in the algorithm causes chattering. A common approach to eliminate chattering is the so-called boundary layer approach, in which the discontinuous function is simply replaced by a continuous function. A problem of this approach is that it does not realize the exact sliding mode, although many previous work (Slotine et al., 1987; Moura et al., 1997; Qiao et al., 2013) employ this approach.

For the numerical integration of differential inclusions, implicit (backward) Euler discretization has been known to be useful to prevent chattering (Kikuuwe et al., 2010; Jin et al., 2012; Acary and Brogliato, 2010; Huber et al., 2016). Not only preventing chattering, as will be illustrated in the following derivation, the implicit Euler discretization preserves the set-valuedness. Due to this fact, what theoretically happens in the continuous-time domain, such as those described in Section 2.3, also happens in the discrete-time domain.

The implicit Euler discretization of (2) can be written as follows:

$$\frac{z_1(k) - z_1(k-1)}{h} = z_2(k) - \alpha_1\sigma(k) - \kappa_1 e_1(k) \tag{30a}$$
$$\frac{z_2(k) - z_2(k-1)}{h} = -\alpha_2\sigma(k) - \kappa_2 e_1(k) \tag{30b}$$
$$w(k) = z_2(k) \tag{30c}$$
$$e_1(k) = z_1(k) - y(k) \tag{30d}$$
$$\sigma(k) \in \eta(e_1(k)) \tag{30e}$$

where k denotes the discrete-time index and $h > 0$ is the time-step size. It is easy to see that the following is obtained.

$$z_1(k) = y(k) + e_1(k) \tag{31a}$$
$$z_2(k) = \frac{z_1(k) - z_1(k-1)}{h} + \kappa_1 e_1(k) + \alpha_1\sigma(k). \tag{31b}$$

This implies that, once $\sigma(k)$ and $e_1(k)$ are obtained, $\{z_1(k), z_2(k)\}$ are obtained. Eliminating $z_1(k)$ and $z_2(k)$ from (30a)(30b)(30d) yields

$$e_1(k) = e^*(k) - B\sigma(k) \tag{32}$$

where

$$D \triangleq 1 + h\kappa_1 + h^2\kappa_2 \tag{33}$$
$$B \triangleq h(\alpha_1 + h\alpha_2)/D \tag{34}$$
$$e^*(k) \triangleq (z_1(k-1) + hz_2(k-1) - y(k))/D \tag{35}$$

and substituting it into (30e) leads to the following:

$$\sigma(k) \in \eta(e^*(k) - B\sigma(k)). \tag{36}$$

To obtain solutions of the algebraic inclusion (36), let us consider the following function:

$$\psi(\xi) \triangleq \{z \in \mathbb{R} \,|\, z \in \eta(B(\xi - z))\}. \tag{37}$$

With this function ψ, (36) can be equivalently rewritten as follows:

$$\sigma(k) = \psi(e^*(k)/B). \tag{38}$$

Because of the properties (3) of η, (37) implies that $\psi(\xi)$ satisfies the following conditions:

$$\psi(\xi) = \xi \quad \forall\xi \in [-1, 1] \tag{39a}$$
$$\lim_{\xi\searrow 1}\psi(\xi) = 1, \ \lim_{\xi\nearrow -1}\psi(\xi) = -1 \tag{39b}$$
$$\psi'(\xi) \ge 0 \quad \forall\xi \in \mathbb{R} \tag{39c}$$
$$\lim_{\xi\to\pm\infty}\psi(\xi)/\xi = 0 \tag{39d}$$
$$\lim_{\xi\searrow 1}\psi'(\xi) = \lim_{\xi\nearrow -1}\psi'(\xi) = 1 \tag{39e}$$
$$\lim_{\xi\to\pm\infty}\psi(\xi) = \pm\infty, \tag{39f}$$

which implies that ψ is a continuous (and also differentiable) function. That is, despite the fact that the algebraic inclusion (36) involves the set-valued function η, its

solution (38) only involves a continuous function. If one chooses $\eta = \mathrm{sgn}$ by neglecting the conditions (3e)(3f), the definition (37) implies that that ψ becomes

$$\psi(\xi) = \mathrm{sat}(\xi) \triangleq \xi / \max(1, |\xi|), \tag{40}$$

which violates (39e) and (39f).

By using (38), the discrete-time algorithm to obtain the numerical solution of the proposed sliding mode differentiator (2) is obtained as follows:

$$e^*(k) := (z_1(k-1) + hz_2(k-1) - y(k))/D \tag{41a}$$
$$\sigma(k) := \psi(e^*(k)/B) \tag{41b}$$
$$e_1(k) := e^*(k) - B\sigma(k) \tag{41c}$$
$$z_1(k) := y(k) + e_1(k) \tag{41d}$$
$$z_2(k) := \frac{z_1(k) - z_1(k-1)}{h} + \kappa_1 e_1(k) + \alpha_1 \sigma(k) \tag{41e}$$
$$w(k) := z_2(k). \tag{41f}$$

Note that (41) is algebraically equivalent to (30) but (41) is free from discontinuities and set-valuedness.

It is not straightforward to obtain ψ from a given η through the definition (37). One approach is to give a closed-form ψ that satisfies (39), which results in its correspondent η satisfying (3). In this approach, η is given only as an implicit function but the closed form of η is not necessary for the implementation. One example of ψ that satisfies (39) is as follows:

$$\psi(\xi) \triangleq \begin{cases} \xi & \text{if } |\xi| \le 1 \\ \mathrm{sgn}(\xi)(\rho|\xi|^{1/\rho} - \rho + 1) & \text{if } |\xi| \ge 1 \end{cases} \tag{42}$$

where ρ is a constant satisfying $\rho > 1$.

The observer algorithm (41) is said to be in the sliding mode when $|e^*(k)| \le B$, which results in $e_1(k) = 0$. A straightforward derivation shows that, if this situation continues for two successive timesteps (i.e., $e_1(k) = e_1(k-1) = 0$), the algorithm (41) reduces to the following:

$$w(k) = \frac{\alpha_1 w(k-1) + \alpha_2 (y(k) - y(k-1))}{\alpha_1 + h\alpha_2}. \tag{43}$$

This is exactly the implicit Euler implementation of $sG_{\mathrm{sm}}(s)$, which appears in (22a). Recall that, as Section 2.3 suggests, the observer (2) reduces to $sG_{\mathrm{sm}}(s)$ in the sliding mode in the continuous time. It has now been shown that the implicit Euler discretization realizes the exact sliding mode also in the discrete time.

It should be emphasized that, because of the absence of the discontinuity, the presented algorithm does not result in chattering irrespective of the fact that the order of sliding mode is only one. It is in contrast to second-order sliding mode approaches, which intend to reduce chattering by hiding the discontinuities in higher-order derivatives. It should also be noted that the computational cost of the algorithm (41) combined with (42) is negligible because everything is in closed form. This feature is in contrast to what a recent work (Efimov et al., 2017) has pointed out regarding the implicit Euler implementation of a second-order sliding mode algorithm.

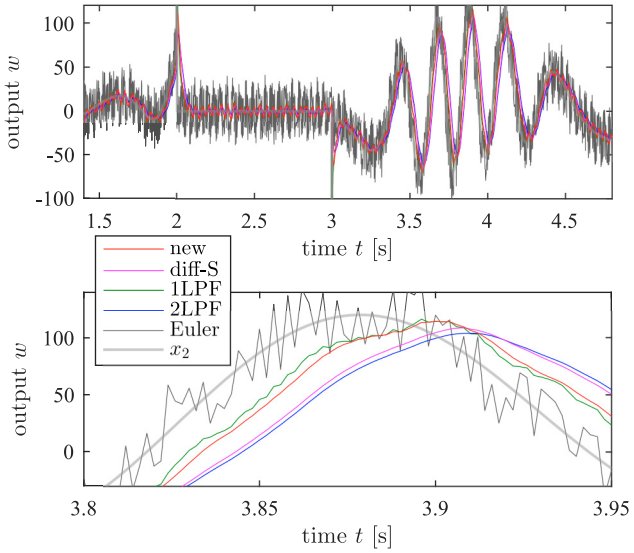

Fig. 2. Results of open-loop simulation. The bottom figure is an enlarged view of the top figure.

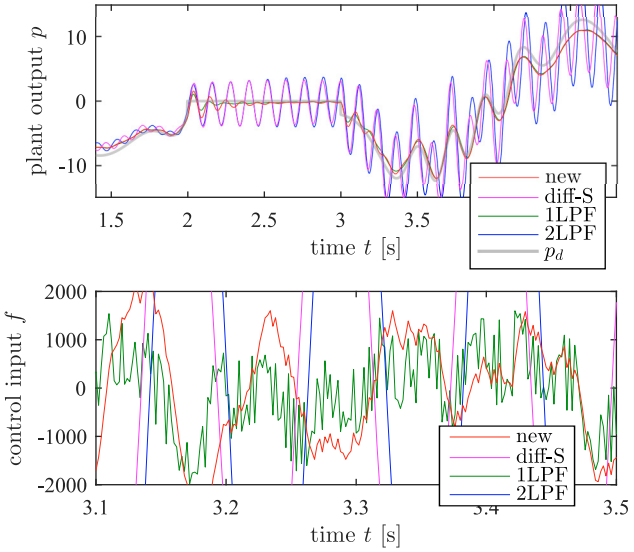

Fig. 3. Results of closed-loop simulation

4. NUMERICAL EXPERIMENTS

The algorithm (41) of the proposed differentiator was experimentally tested. Two sets of simulations, open-loop and closed-loop, were performed. The timestep size was set as $h = 0.002$ s. For the comparison, the following differentiators were used:

- **new**: The proposed algorithm (41) with the parameter settings (29) with $\omega_{\mathrm{sm}} = \omega_{\mathrm{far}} = 20\pi$ rad/s, $\gamma = 5$, and η defined by (42) and $\rho = 4$.
- **diff-S**: The proposed algorithm (41) with the same setting as **new** except $\eta = \mathrm{sgn}$. This can be seen as the implicit Euler implementation of Slotine et al.'s observer applied to the integrator (1).
- **1LPFs**: First-order Euler differentiation plus the first-order LPF, $sG_{\mathrm{sm}}(s)$ with $\omega = \omega_{\mathrm{sm}}$.
- **2LPFs**: First-order Euler differentiation plus a second-order LPF, $sG_{\mathrm{far}}(s)$ with $\omega = \omega_{\mathrm{sm}}$.

In the open-loop simulation, we used the "true" signal x_1 artificially generated by combining some sinusoidal functions and constants. The input signal y was generated as $y := x_1 + v$ where v was a noise signal obtained from a real hardware, a capacitive six-axis force sensor under zero load. Fig. 2 shows the results. It can be seen that the new differentiator is less noisy than 1LPF as well as diff-S and 2LPF, but its phase lag is much smaller than diff-S and 2LPF. This shows an advantage of the new differentiator.

In the closed-loop simulation, the plant was chosen as the following third order system:

$$\mathcal{L}[p] = \mathcal{L}[f]/(As^3 + Ms^2 + Bs) \tag{44}$$

where f and p are the input and the output of the plant, respectively, and $A = 0.01$, $M = 0.5$ and $B = 10$. The measurement was obtained as $y_o = p + v$ where v is the same one as the above. To compensate the phase lag caused by the differentiator, the input signal y to the differentiator was set as

$$y_k = y_{o,k} + (y_{o,k} - y_{o,k-1})/(h\omega_n) \tag{45}$$

where $\omega_n = 2\omega_{\rm sm}$. The controller was constructed as

$$f = K_p(p_d - y_o) + K_d(\dot{p}_d - w) \tag{46}$$

where w is the output of the differentiator and $K_p = 100$ and $K_d = 50$.

Fig. 3 shows the results of closed-loop simulation. This indicates that diff-S and 2LPF produced oscillatory (nearly unstable) behaviors but 1LPF and the new differentiator resulted in stable tracking, although the output of the new one is slightly more oscillatory than 1LPF. The data of f shows that the control input f is noisier with 1LPF than the new differentiator. This shows that the new differentiator is effective for realizing better stability and lower noisiness than the other methods.

5. CONCLUSIONS

This paper has presented a new sliding mode differentiator for estimating the first-order derivatives of noisy signals. The differentiator is a first-order sliding mode system, which can be seen as a non-Lipschitz variant of Slotine et al.'s (1987) sliding mode observer. The paper has also analyzed the proposed differentiator based on its analytical relations to linear LPFs and showed the global asymptotic and input-to-state stability. In addition, the paper has provided a discrete-time implementation of the proposed differentiator based on the implicit Euler discretization, which does not produce chattering and realizes the exact sliding mode. The proposed algorithm was tested through numerical examples.

Future research should address better guidelines for parameter tuning, especially about γ, and the design of the function ψ. A more in-depth analysis to clarify the relation with higher-order sliding mode systems such as Levant's (2003) differentiator, considering the homogeneity issues (e.g., Cruz-Zavela and Moreno, 2017; Angulo et al., 2013), is also subject to future studies.

REFERENCES

Acary, V. and Brogliato, B. (2010). Implicit Euler numerical scheme and chattering-free implementation of sliding mode systems. *Systems & Control Letters*, 59(5), 284–293.

Angulo, M.T., Moreno, J.A., and Fridman, L. (2013). Robust exact uniformly convergent arbitrary order differentiator. *Automatica*, 49, 2489–2495.

Cortés, J. (2008). Discontinuous dynamical systems. *IEEE Control Systems*, 28(3), 36–73.

Cruz-Zavela, E. and Moreno, J.A. (2017). Homogeneous high order sliding mode design: A Lyapunov approach. *Automatica*, 80, 232–238.

Davila, J., Fridman, L., and Levant, A. (2005). Second-order sliding-mode observer for mechanical systems. *IEEE Trans. Automatic Control*, 50(11), 1785–1789.

Efimov, D., Polyakov, A., Levant, A., and Perruquetti, W. (2017). Realization and discretization of asymptotically stable homogeneous systems. *IEEE Trans. Automatic Control*.

Huber, O., Acary, V., Brogliato, B., and Plestan, F. (2016). Implicit discrete-time twisting controller without numerical chattering: Analysis and experimental results. *Control Engineering Practice*, 46, 129–141.

Iqbal, M., Bhatti, A.I., Ayubi, S.I., and Khan, Q. (2010). Robust parameter estimation of nonlinear systems using sliding-mode differentiator observer. *IEEE Trans. Industrial Electronics*, 58(2), 680–689.

Jin, S., Kikuuwe, R., and Yamamoto, M. (2012). Real-time quadratic sliding mode filter for removing noise. *Advanced Robotics*, 26(8-9), 877–896.

Kikuuwe, R., Yasukouchi, S., Fujimoto, H., and Yamamoto, M. (2010). Proxy-based sliding mode control: A safer extension of PID position control. *IEEE Trans. Robotics*, 26(4), 860–873.

Levant, A. (1998). Robust exact differentiation via sliding mode technique. *Automatica*, 34(3), 379–384.

Levant, A. (2003). Higher-order sliding modes, differentiation and output-feedback control. *Int. J. Control*, 76(9/10), 924–941.

Levant, A. and Livne, M. (2012). Exact differentiation of signals with unbounded higher derivatives. *IEEE Trans. Automatic Control*, 57(4), 1076–1080.

Moura, J.T., Elmali, H., and Olgac, N. (1997). Sliding mode control with sliding perturbation observer. *Trans. ASME: J. Dynamic Systems, Measurement, and Control*, 119, 657–665.

Qiao, Z., Shi, T., Wang, Y., Yan, Y., Xia, C., and He, X. (2013). New sliding-mode observer for position sensorless control of permanent-magnet synchronous motor. *IEEE Trans. Industrial Electronics*, 60(2), 710–719.

Slotine, J.J.E., Hedrick, J.K., and Misawa, E.A. (1987). On sliding observers for nonlinear systems. *Trans. ASME: J. Dynamic Systems, Measurement, and Control*, 109(3), 245–252.

Vasiljevic, L.K. and Khalil, H.K. (2008). Error bounds in differentiation of noisy signals by high-gain observers. *Systems and Control Letters*, 57(10), 856–862.

Vázquez, C., Aranovskiy, S., Freidovich, L.B., and Fridman, L. (2016). Time-varying gain differentiator: A mobile hydraulic system case study. *IEEE Trans. Control Systems Technology*, 24(5), 1740–1750.